

LOADING OF CLARITHROMYCIN AND PACLITAXEL ON SYNTHESIZED CDS/NIO NANOPARTICLES AS PROMISING NANOCARRIERS

MUSTAFA R. ABDULBAQI¹, NIDHAL K. MARAIE¹, ASHOUR H. DAWOOD²

¹Department of Pharmaceutics, College of Pharmacy, Al-Mustansiriya University, Baghdad, Iraq, ²Department of pharmaceutical chemistry, College of Pharmacy, Al-Mustansiriya University, Baghdad, Iraq
Email: dr_nidhal_khazaal@yahoo.com

Received: 17 Feb 2016 Revised and Accepted: 30 Mar 2016

ABSTRACT

Objective: In this study cadmium sulfide (CdS) and nickel oxide (NiO) nanoparticles were synthesized and applied as novel nanocarriers for antibacterial drug clarithromycin (CLA) and anticancer drug paclitaxel (PTX) to improve their physical properties and biological activities.

Methods: Cadmium sulfide (CdS) and nickel oxide (NiO) nanoparticles were synthesized by chemical co-precipitation and thermochemical processing techniques respectively and loaded with clarithromycin (CLA) and paclitaxel (PTX) by simple new one-step reaction. Analytical measures including FTIR, PXRD, SEM, AFM, TGA, DSC and zeta potential were used for characterization. The *in vitro* release, antibacterial as well as anticancer activities were evaluated.

Results: Analytical measures revealed that the loading involved physical complex formation rather than chemical modification with the high percent surface loading of the drugs on the nanoparticles. Solubility/dissolution study revealed higher significant* improvement in the solubility of CLA from NiO nanoparticles than that from CdS nanoparticles while the antibacterial activity of CLA was non-significantly improved. For PTX loaded on CdS and NiO nanoparticles showed non-significant change in its solubility, but remarkable significant* increase in its antitumor activity on MCF-7 cell line accompanied with significant* reduction in its cytotoxicity on normal mammary cell line (MCF-10A) indicating the selectivity and targeting of PTX-CdS/NiO nanocarriers with reduced side effects of the drug and the used metal nanocarriers.

Conclusion: This work provided most selective and safe delivery system for PTX and best method for enhancement of CLA solubility.

Keywords: Clarithromycin (CLA), Paclitaxel (PTX), Cadmium sulfide (CdS) nanoparticles, Nickel oxide (NiO) nanoparticles

© 2016 The Authors. Published by Innovare Academic Sciences Pvt Ltd. This is an open access article under the CC BY license (<http://creativecommons.org/licenses/by/4.0/>)

INTRODUCTION

Nanocarriers are nanomaterials being used as transport modules for another substance such as drugs [1]. Nanocarriers with improved biological and physicochemical properties are taken up by cells more easily than larger molecules, so they can be successfully used as delivery tools for currently available bioactive compounds [2]. Among nanoparticles with biomedical advantages are inorganic nanoparticles which include metals (gold, copper, silver, magnesium and iron), metal oxides (iron oxide, zinc oxide, titanium dioxide and cerium oxide) and quantum dots (cadmium selenide and cadmium sulfide) [3]. Metal NPs are unique with various biomedical applications involving drug and gene delivery, highly sensitive diagnostic assays, radiotherapy enhancement and thermal ablation [4]. Nickel oxide (NiO) is an important metal oxide that has been applied in the medical field and as a catalyst in magnetic recording media as well as its cytotoxic and anticancer activity [5, 6].

Quantum dots (QDs) are nanocrystalline semiconductors with unique optical and electronic properties [7]. Cadmium sulfide (CdS) nanocrystals are QDs that have the advantages of high photostability, high quantum yield, bio-imaging of living cells and as a fluorescence probe for the rapid determination of DNA [8, 9]. In spite of its cytotoxicity, cadmium is the main component in most QDs which cadmium inhibit DNA, RNA and proteins synthesis, DNA strands breaking and chromosomes mutation [10]. In addition CdS nanoparticles decrease the viability of HeLa cells with increased NPs concentration as well as the cell division expression of *E. coli* was decreased when exposed to CdS nanoparticles [11].

Paclitaxel (Taxol) is a widely used chemotherapeutic drug, it is a FDA-approved drug for the treatment of ovarian cancers, breast, lungs and AIDS related Kaposi's sarcoma [12]. Paclitaxel acts by promotion of microtubules stabilization and induce cytotoxic effect by increased reactive oxygen species (ROS) and reactive nitrogen species (RNS) production [13]. Paclitaxel is BCS class IV drug with

poor solubility and poor permeability [14], in which the high lipophilicity with very poor aqueous solubility of less than 0.01 mg/ml as well as lack of ionizable functional groups are the major challenges in the paclitaxel dissolution and delivery [15].

Clarithromycin (CLA) is a macrolide antibiotic that is indicated widely for the treatment of *H. pylori* mediated peptic ulcers as well as Upper Respiratory Tract Infections (URT) [16], it acts by binding to the 50S ribosomal subunit of susceptible organisms and thereby inhibiting protein synthesis through translocation of aminoacyl transfer RNA [17]. CLA have a dissolution rate-limited absorption and low bioavailability after oral administration due to its low solubility in which CLA belongs to the class II of BCS [18].

This work involves the preparation and application of CdS and NiO nanoparticles as nanocarriers for clarithromycin and paclitaxel through simple one step reaction that may contribute to improvement in solubility, dissolution, permeability and their therapeutic activities as well as reducing their undesirable and adverse effects of the medically applied metals.

MATERIALS AND METHODS

Materials

Paclitaxel and clarithromycin were provided by JIANGSU YEWE PHARMACEUTICAL Co. Limited (China), sodium sulfide (Na₂S. xH₂O) was obtained from THOMAS BAKER Co. Limited (India), cadmium acetate dihydrate (CH₃COO)₂Cd.2H₂O was obtained from Qualikems Fine Chem Co. Ltd. (India), nickel nitrate Ni(NO₃)₂.6H₂O was obtained from Barcelona Co. Limited (Spain), ammonia solution NH₄(OH) and acetonitrile C₂H₃N were obtained from Sinopharm Chemical Reagent Co. Limited (China), acetone C₃H₆O and ethanol C₂H₆O were obtained from Sigma Chemical Co. Limited (USA) and dimethyl sulfoxide (DMSO) was obtained from Loba Chemie Pvt. Ltd (India).

Methods

Synthesis of cadmium sulfide (CdS) and nickel oxide (NiO) nanoparticles

Cadmium Sulphide (CdS) nanoparticles were synthesized by chemical co-precipitation technique. This method involved drop wise titration (10 drops/min) of 0.1 M aqueous solution disodium sulfide onto 0.1 M aqueous solution cadmium acetate dihydrate with vigorous stirring (1500 rpm) and heating at 50 °C by a magnetic stirrer (Dragon Lab, USA). While dropping and stirring, the solution color change from yellow to orange, then red and finally return back to orange color. After dropping has been finished, the vigorous stirring (1500 rpm) is continued and temperature hold constant at 50 °C for 4 h. Then the produced yellow-orange particles (final product) was filtered, washed with deionized water and desiccated within silica gel containing desiccator for three days and collected [19]. Nickel Oxide (NiO) NPs were synthesized by thermochemical processing method. This technique involved dropwise titration of 100 ml ammonium hydroxide solution (10 drops/min) onto preheated 0.5 M nickel nitrate aqueous solution to 70 °C with vigorous stirring (1500 rpm). As dropping has been completed, the vigorous stirring is continued, and the temperature kept at 70 °C for 4 h and then filtered. The obtained light green residue was then washed with 1:1 (v/v) ethanol and deionized water and heated in an oven (Mettler, Germany) to 70 °C for 24 h followed by 220 °C for 2 h resulting in black nanoparticles of NiO [20, 21].

Loading of clarithromycin and paclitaxel on CdS nanoparticles

Clarithromycin and Paclitaxel each one separately was loaded to CdS nanoparticles by incorporation method which involves the addition of the drug in the last step of nanoparticles synthesis, where 0.1 M of clarithromycin using acetone as a solvent and 0.1 M of paclitaxel using acetonitrile as a solvent was added (each one separately) by fast dropping to the mixture of cadmium acetate and sodium sulfide while it is vigorously stirred (1500 rpm) at 50 °C and just before dropping of sodium sulfide has been finished. After finishing the sodium sulfide dropping, the stirring was continued for 4 h and then filtered, washed with ethanol, desiccated and finally collected as a light yellow powder to be characterized and evaluated [22].

Loading of clarithromycin and paclitaxel on NiO nanoparticles

Loading of clarithromycin and Paclitaxel each one separately on NiO nanoparticles was done by (Adsorption/Absorption) method that involves addition of 0.1 M of each drug by fast dropping to the preheated solution of NH₄OH containing NiO nanoparticles at 60 °C with vigorous stirring (1500 rpm) that continued for 2 h after drug addition had been completed. Then the mixture is filtered, washed with ethanol to remove impurities, desiccated and finally collected as a grey powder to be characterized and evaluated [23].

Characterization of clarithromycin and paclitaxel-loaded CdS and NiO nanoparticles

Fourier Transform Infra-red spectroscopy (FTIR)

Fourier Transform Infra-Red spectroscopy (FTIR) instrument (Shimadzu Japan) was used to determine the nature of associated functional groups, and it was employed for pure clarithromycin, pure paclitaxel, CdS nanoparticles loaded clarithromycin, CdS nanoparticles loaded paclitaxel, NiO nanoparticles loaded clarithromycin and NiO nanoparticles loaded Paclitaxel by FTIR spectroscopy (4000-500 cm⁻¹) using potassium bromide disc [24].

Powder X-ray diffraction (PXRD)

PXRD was achieved for pure drugs, nanoparticles alone and nanoparticles loaded drugs to determine their crystallinity, in which the PXRD instrument (Shimadzu, Japan) was equipped with Cu-Kα radiation (λ = 1.54060 Å), voltage (40 Kv) and current (30 mA). The samples were analyzed in scanning speed of (5 °/min) and axis θ-2θ with a range of 5 to 60 degrees [25].

Scanning electron microscope (SEM)

Scanning electron microscope instrument (FET company, Netherlands) is used to determine the shape, size and morphologies

of formed nanoparticle to give high-resolution images of the sample surface by magnifying images up to 200,000 times [26]. Sample (1-2 mg) of produced nanoparticles before and after loading with drugs as well as for pure drugs was mounted on the small aluminum holder and coated with gold, then introduced into SEM instrument and scanned with a fine focused beam of electrons to take images [27].

Zeta potential

Zeta (ξ) potential analysis was applied for CdS and NiO nanoparticles before and after loading with clarithromycin and paclitaxel as well as for free drugs as an indicator of their stability in suspension and was performed by dissolving 2 mg of each sample separately in 10 ml of phosphate buffer PH 7.4 with sonication, then filtered with 0.2 μl filter syringe and finally introduced to the zeta potential analyzer (Brookhaven, USA) to read the zeta potential data for each sample [28].

Thermal gravimetric analysis (TGA)

Powder samples of pure drug, CdS and NiO nanoparticles and nanoparticles loaded drugs were analyzed by TGA to evaluate their thermal behavior during heating process (25-600 °C), in which 20 mg of each sample was located separately in TG instrument (Linseis, Germany) pan so that record the weight loss with increase temperature by subjecting them to a constant heating rate of 5 °C/min and nitrogen atmosphere with a gas flow of 50 ml/min. As a result, the thermal scan was recorded as plot of heat flow versus temperature [29, 30].

Differential scanning calorimetric (DSC)

Differential scanning calorimetric analysis (Linseis, Germany) was carried out for pure drugs, CdS and NiO nanoparticles and nanoparticles loaded drugs by taking 10 mg of each sample and dispersed in 5 ml of phosphate buffer PH 7.4, then take 1 ml of the dispersed sample and heated from 25 °C to 300 °C at the rate of 10 °C/min and under a carrier of nitrogen gas supplied at 10 mL/min [31].

Atomic force microscopy (AFM)

Atomic Force Microscopy (Augustrom advance Inc., USA) was used to determine the shape, size and size distribution of nanoparticles by resolving individual particles and groups of particles in three dimensions analysis [32] and it was performed for pure drugs, CdS and NiO nanoparticles and nanoparticles loaded drugs. Powder samples were dissolved in methanol, and few drops of each sample were dropped separately on a silica glass plate and allowed to dry at room temperature to be deposited on the plate. The deposited film was then scanned with the Atomic Force Microscopy instrument [33].

Calculations of drug yield, drug entrapment efficiency, and drug loading percentages

The percentage of yield was calculated as a percentage ratio of the weight of nanoparticles (or materials forming it) after incorporation of the drug with nanoparticles to the weight of nanoparticles and drug fed initially in the reaction before incorporation and as follows:

$$\% \text{ yield} = \frac{\text{weight of nanoparticles after drug incorporation(actual)}}{\text{weight of nanoparticles and drug before incorporation(theoretical)}} \times 100\%$$

The percentage of entrapment efficiency (% e. e) of the drug was calculated as a percentage ratio of the weight of drug in nanoparticles after incorporation to the weight of drug fed initially in the reaction before incorporation and as follows:

$$\% \text{ e. e} = \frac{\text{weight of drug in nanoparticles after incorporation(actual)}}{\text{weight of drug fed initially before incorporation(theoretical)}} \times 100\%$$

The percentage of drug loading was calculated as a percentage ratio of the weight of drug in nanoparticles alone to the weight of nanoparticles loaded with the drug and as follow [34, 35]:

$$\% \text{ drug loading} = \frac{\text{weight of drug in nanoparticles}}{\text{weight of nanoparticles loaded with the drug}} \times 100\%$$

In vitro drugs release study

Clarithromycin *in vitro* release study from the prepared nanocarriers was achieved using USP type II rotating paddle apparatus (Copley, UK) at (37±0.5 °C) and the rotating speed of 50 rpm in 500 ml of phosphate buffer solution (pH 7.4). Equivalent to 100 mg CLA of the prepared CdS and NiO nanoparticles loaded with CLA as well as 100 mg of standard CLA were dispersed in the dissolution medium, and samples of 5 ml were withdrawn at predetermined time intervals and replaced with the same volume of fresh media after each withdrawal, then the withdrawn samples were filtered and the content of CLA was determined spectrophotometrically by using UV-Visible spectrophotometer (Shimadzu, Japan) at 210 nm, each experiment was analyzed in triplicate [36, 37].

The same was applied to paclitaxel by dispersing 10 mg of the standard PTX as well as equivalent to 10 mg PTX of the prepared CdS and NiO nanoparticles loaded with PTX in 500 ml of phosphate buffer solution PH 7.4 using USP type II rotating paddle apparatus (Copley, UK) at (37±0.5 °C) and rotating speed of 50 rpm. The withdrawn samples were determined spectrophotometrically by using UV-Visible spectrophotometer (Shimadzu, Japan) at 230 nm; each sample was analyzed in triplicate [38].

Solubility determination of drugs before (free drug) and after loading with nanoparticles

A widely spread method to determine the equilibrium solubility of drug molecules is saturation shake-flask method. An excess amount of CLA (10 mg/ml), PTX (0.1 mg/ml) and an equivalent amount of each drug loaded CdS and NiO nanoparticles were dispersed separately in phosphate buffer PH 7.4 containing stoppered flask in a water bath at 37 °C and stirred by magnetic stirrer (Dragon Lab, USA) for 48 h. After 48 h the undissolved material was filtered, and the concentration of dissolved drug was quantified using UV-Visible spectrophotometer (Shimadzu, Japan) at the specified λ max of each drug in triplicate [39].

Antibacterial activity test of clarithromycin loaded nanoparticles

The antibacterial biological activity of clarithromycin loaded CdS and NiO nanoparticles each separately was compared with free CLA as well as with blank CdS and NiO nanoparticles. Each sample was tested against two types of Gram+ve bacteria (*Staphylococcus aureus* and *Streptococcus pyogenes*) and two types of Gram-ve bacteria (*Serratia marcescens* and *Klebsiella oxytoca*) at concentration 100 µg/ml of free CLA and an equivalent concentration of CLA loaded with CdS and NiO nanoparticles as well as blank CdS and NiO nanoparticles. The samples were dissolved using dimethyl sulfoxide (DMSO) as a solvent and cultured in Muller Hinton agar for 24 h at 37 °C [40, 41].

Antitumor activity of paclitaxel-loaded nanoparticles

The antitumor activity of paclitaxel before and after loading with CdS and NiO nanocarriers as well as of blank CdS and NiO nanoparticles was performed by Centre for Natural Products Research and Drug Discovery in the University of Malaya using the following procedures:

Cell culture

The human cancer breast cell line (MCF-7) and human mammary epithelial cell line (MCF-10A) were grown each separately in Dulbecco modified Eagle's medium (DMEM) with 10% (v/v) heat-inactivated newborn calf serum and antibiotics (100 mg/ml of streptomycin and 100 U/ml of penicillin) at 37 °C in a humidified atmosphere containing 5% CO₂ [42].

MTT assay

MCF-7 cells and MCF-10A cells were seeded separately in a 96-well plate (0.8×10⁴ cells/well) in triplicate and incubated for 24 h to be attached to the plates. After incubation for 24 h, cells were treated with increasing concentrations (2.5, 5, 10, 20 nM) of pure paclitaxel, paclitaxel loaded CdS and NiO nanoparticles and blank CdS and NiO nanoparticles for 24, 48 and 72 h respectively [43, 44]. After

respective incubation periods, 20 µl (5 mg/ml) of MTT (3-(4,5-Dimethylthiazol-2-yl)-2,5-Diphenyltetrazolium Bromide) was added to each well and incubated for 4 h at 37 °C. Then the formazan crystals formed by the viable cells were dissolved by the addition of 200 µl of DMSO to each well, and the color intensity value of the processed cells was measured at 550 nm that presents the cell survival percentage in corresponding wells in contrast with their respective controls [42, 45].

Statistical analysis

All the experiments were conducted in triplicates, and the comparisons of quantitative data obtained from antibacterial and antitumor activity of clarithromycin and paclitaxel respectively were analyzed using one-way, and two-way ANOVA tests, as well as Student T-test, was used for clarithromycin quantitative data comparison for *in vitro* release, the results were expressed as mean±standard deviation. Statistical analysis was performed using the statistical package SPSS for windows (version 13, SPSS Inc., Chicago, IL, USA). The statistical significance for each test a *P* value of less than 0.05 was adopted.

RESULTS

Synthesis of cadmium sulfide (CdS) and nickel oxide (NiO) nanoparticles

The reaction of 0.1 M of sodium sulfide Na₂S with 0.1 M of cadmium acetate (CH₃COO)₂Cd in special conditions resulted in an orange precipitated nanoparticles of cadmium sulfide (CdS) according to the following equation [46]:

$$\text{Na}_2\text{S} + \text{Cd}(\text{CH}_3\text{COO})_2 \rightarrow \text{CdS}(\text{NPs})\downarrow + (2\text{CH}_3\text{COONa})$$

The reaction of 0.5 M of Nickel nitrate Ni(NO₃)₂·6H₂O with ammonium hydroxide NH₄OH with vigorous stirring (1500 rpm) and heating (70 °C) for 4 h, followed by heating in the oven for 24 h with 70 °C, after that rise the temperature in the oven up to 220 °C for 2 h to calcify the product resulted in black precipitate of nickel oxide nanoparticles as displayed in following equation [47]:



Loading of the drugs on CdS and NiO nanoparticles

The drugs are believed to be loaded on cadmium sulfide (CdS) nanoparticles by physical complexation without any chemical reaction, in which a yellow powder was obtained for both CLA and PTX loaded CdS nanoparticles as a new compound that differ from the original color of CLA (white) and PTX (white) as well as from the original color of CdS nanoparticles (orange) resulting from complex formation between the drugs and the nanocarrier. The loading of clarithromycin and paclitaxel on nickel oxide (NiO) nanoparticles (black nanoparticles) was obtained as a grey powder resulting from the complexation of the drugs with nanoparticles by physical attraction.

Characterization of clarithromycin and paclitaxel-loaded CdS and NiO nanoparticles

Furrier transform infra-red (FTIR)

The FTIR spectrum (fig. 1) of clarithromycin displays bands at the range (3618–3420 cm⁻¹) attributed to multiple hydroxyl groups (OH) in the backbone structure of CLA. The bands at 1722 cm⁻¹ and 1697 cm⁻¹ assign to the two carbonyl groups of ester and ketone respectively, while the aliphatic groups (CH₃ and CH₂) were appeared in the expected area for the stretching (asymmetrical and symmetrical) in the range (1990–2781 cm⁻¹) while the finger prints area shows the bending bands of the drug. The FTIR spectrum of CLA loaded CdS nanoparticles, and CLA loaded NiO nanoparticles shows the OH and other groups appeared in the same values with that of free CLA with small shifting. The FTIR spectrum of paclitaxel shows peaks at 3510 cm⁻¹ and 3439 cm⁻¹ can be attributed to stretching of a hydroxyl group (OH) in two different environments; the amidic group was shown at 3350 cm⁻¹. The bands at 3063 cm⁻¹ and 3021 cm⁻¹ assign to aromatic CH stretching, while the carbonyl groups appear as multiband due to the different environments of these groups at 1712, 1700, 1647 and 1602 cm⁻¹. The FTIR spectrum of loaded drug (PTX) with CdS and NiO nanoparticles appeared with the same functional groups of free PTX with small shifting.

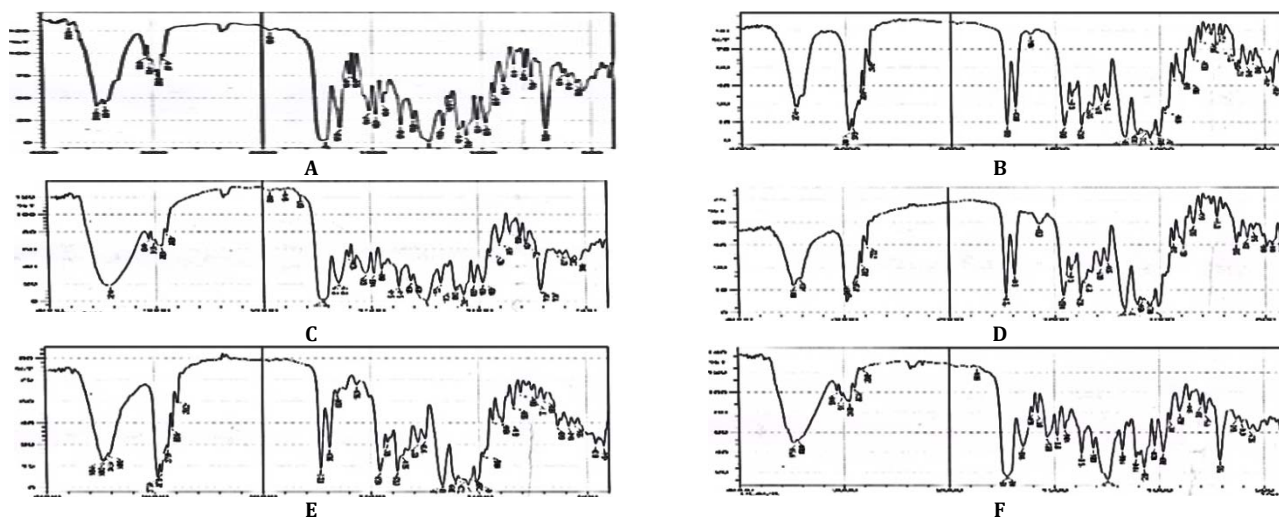


Fig. 1: FTIR of (A) pure clarithromycin, (B) pure paclitaxel, (C) CLA loaded CdS nanoparticles, (D) PTX loaded CdS nanoparticles, (E) CLA loaded NiO nanoparticles and (F) PTX loaded NiO nanoparticles. CLA: clarithromycin; PTX: paclitaxel; CdS: cadmium sulfide; NiO: nickel oxide

X-Ray diffraction (XRD)

The X-Ray Diffraction (XRD) spectrum (fig. 2) of blank CdS and NiO nanoparticles displays sharp, intense peaks with high multiplicity indicating crystalline property. The XRD spectrum of free clarithromycin displays numerous narrow strongly intense diffraction peaks indicating its highly stable crystalline structure, while the XRD of CLA loaded on CdS and NiO nanoparticles show less intense and less characterized sharp diffraction peaks with

decreased multiplicity in comparison with the XRD of free CLA referring to the more amorphous compound. The XRD spectrum of free paclitaxel displays many characterized narrow sharp diffraction peaks indicating PTX crystalline structure, while the XRD spectrum after loading of PTX on CdS and NiO nanoparticles displays increased multiplicity of sharp diffraction peaks with higher intensities in general except some characteristic peak of free PTX referring to enhanced crystalline property of PTX loaded nanocarriers in comparison with the free PTX.

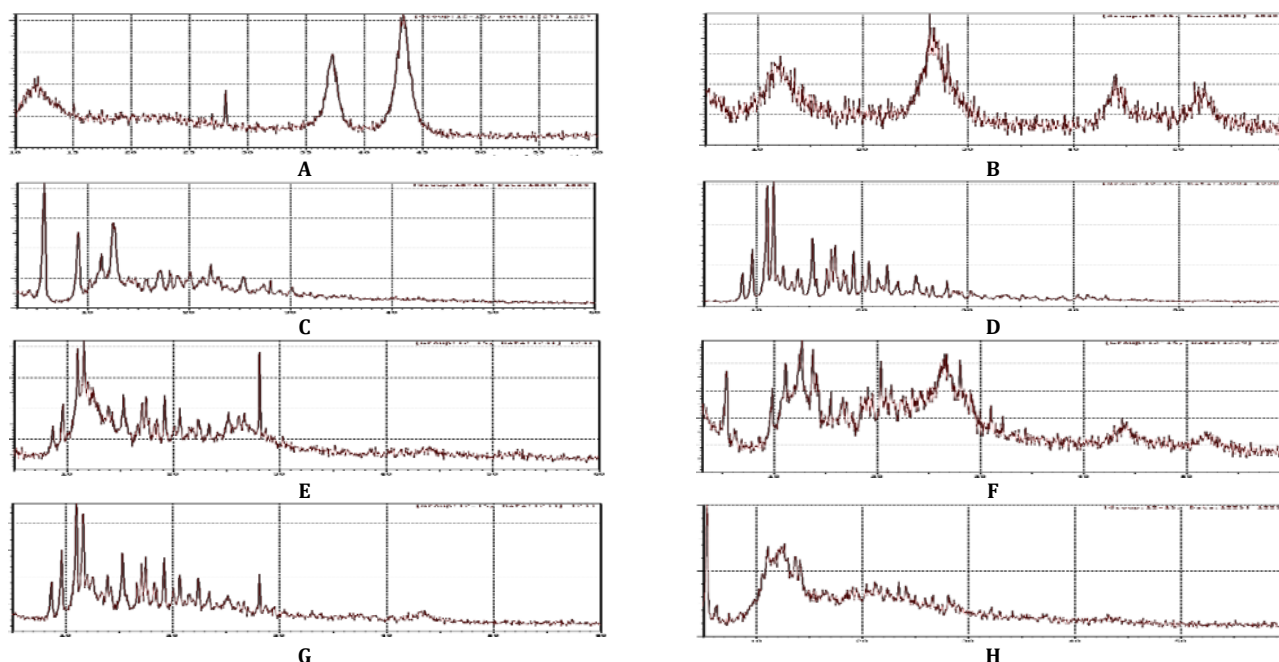


Fig. 2: XRD of (A) blank CdS nanoparticles, (B) blank NiO nanoparticles, (C) pure clarithromycin, (D) pure paclitaxel, (E) CLA loaded CdS nanoparticles, (F) PTX loaded CdS nanoparticles, (G) CLA loaded NiO nanoparticles and (H) PTX loaded NiO nanoparticles. CLA: clarithromycin; PTX: paclitaxel; CdS: cadmium sulfide; NiO: nickel oxide

Scanning electron microscopy (SEM)

The scanned electronic microscope (SEM) images (fig. 3) of loaded clarithromycin with CdS and NiO nanoparticles display different shape and size in comparison with the free CLA and blank CdS and NiO nanoparticles, in which these complexes of

loaded drug appeared more distributed as well as more compact with smoother surfaces. The same changes were observed with the SEM images of paclitaxel after loading with CdS and NiO nanoparticles as they appeared more compact with smoothly fine surfaces than that of free PTX with flakes like shape for PTX-NiO complex.

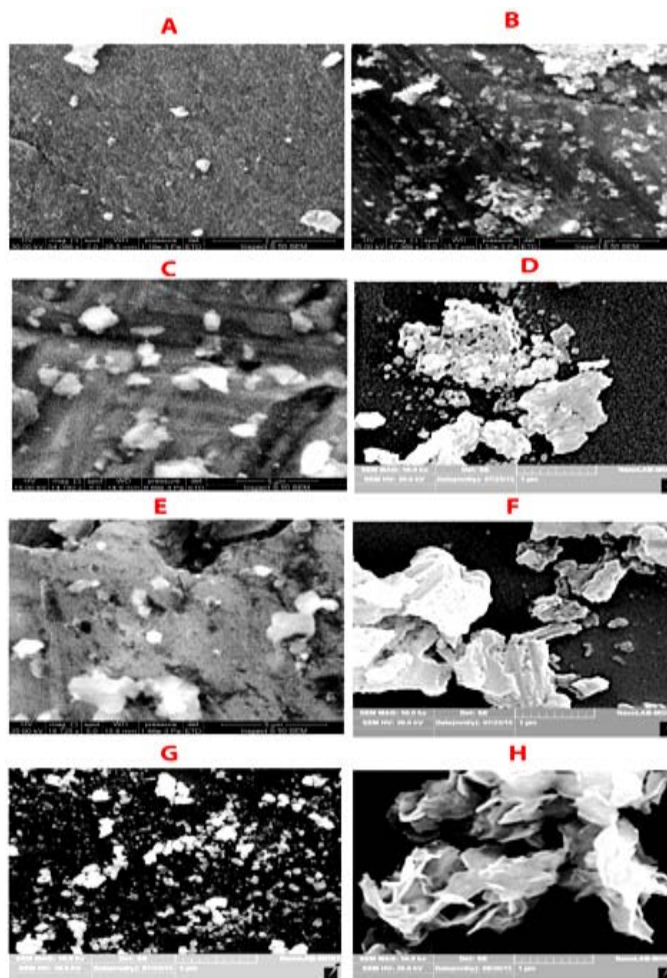


Fig. 3: SEM of (A) blank CdS nanoparticles, (B) blank NiO nanoparticles, (C) pure clarithromycin, (D) pure paclitaxel, (E) CLA loaded CdS nanoparticles, (F) PTX loaded CdS nanoparticles, (G) CLA loaded NiO nanoparticles and (H) PTX loaded NiO nanoparticles. CLA: clarithromycin; PTX: paclitaxel; CdS: cadmium sulfide; NiO: nickel oxide

Table 1: Zeta potential of CdS and NiO nanoparticles before and after loading with clarithromycin and paclitaxel as well as pure drugs

Sample	Zeta Potential (mV)±SD	Mobility(μ/s)/(V/cm)±SD	Frequency (Hz)±SD	Frequency Shift (Hz)±SD
Cds nanoparticles	-152.45±4.8	-3.03±0.10	223.44±0.62	-27.04±0.95
NiO nanoparticles	-90.82±4.1	-1.80±0.08	235.03±0.64	-16.84±1.71
Pure clarithromycin	-119.67±8.23	-2.38±0.16	230.45±1.26	-19.25±4.51
Clarithromycin loaded CdS nanoparticles	-32.54±2.1	-2.15±0.16	232.04±1.48	-16.70±2.81
Clarithromycin loaded NiO nanoparticles	-59.58±6.94	-1.18±0.14	240.65±1.10	-7.68±1.83
Pure paclitaxel	-77.76±4.08	-1.54±0.08	237.13±0.67	-13.98±1.57
Paclitaxel loaded CdS nanoparticles	-117.90±8.95	-2.34±0.18	231.57±1.44	-18.84±1.69
Paclitaxel loaded NiO nanoparticles	-72.93±2.85	-1.45±0.06	238.44±0.46	-11.78±1.65

Data represent mean(±SD) (n=3). CdS: cadmium sulfide; NiO: nickel oxide.

Zeta potential

The zeta potential values are summarized in (table 1) and indicate good stability of clarithromycin loaded CdS and NiO nanoparticles (below -30 mV). The zeta potential of paclitaxel is loaded CdS and NiO nanoparticles display excellent stability (below -60 mV) against aggregation [48].

Thermogravimetric analysis (TGA)

Thermo Gravimetric Analysis (TGA) spectrum (fig. 4) of the prepared blank CdS nanoparticles shows a peak at 398.8 °C indicating its degradation after this temperature while the TGA of

blank NiO nanoparticles shows its degradation peak at 399 °C. Thermal analysis of free clarithromycin shows a peak at 279 °C that is corresponding with the melting of CLA and decomposition of the compound after this degree. Thermal analysis of CLA loaded CdS nanoparticles shows peak at 255.5 °C referring to initiation of decomposition (weight loss) of the CLA-CdS complex followed by degradation above this degree, while CLA loaded NiO nanoparticles thermal analysis shows thermal peak at 276 °C indicating loss of drug by melting since it is close to the melting of free CLA and followed by its decomposition above this temperature. Thermal analysis of paclitaxel shows sharp thermal peak at 230.9 °C that is related to the PTX melting since the drug decompose above this

temperature, while thermal analysis of PTX loaded CdS nanoparticles shows broad weight loss thermal peak at 213.8 °C that result from partial drug decomposition at this peak followed by stationary thermal stability without degradation of PTX-CdS complex, while the paclitaxel loaded NiO thermal analysis displays

two steps of weight loss by thermal effect, first thermal peak appears at 229.6 °C indicating the melting of PTX since it is close to the melting of free drug and followed by decomposition of PTX, while the second thermal peak appears at 359.8 °C that results from degradation of most of the carrier (NiO nanoparticles).

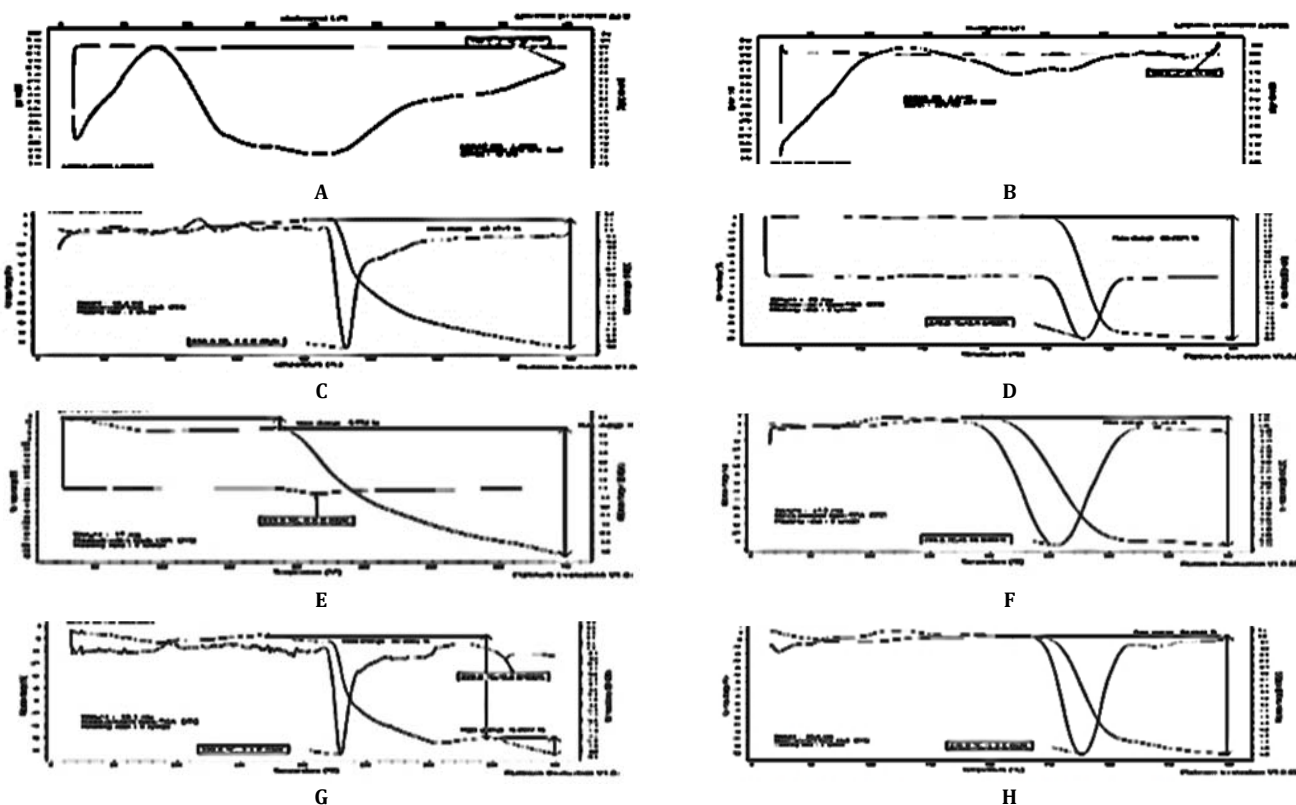


Fig. 4: TGA of (A) blank CdS nanoparticles, (B) blank NiO nanoparticles, (C) pure clarithromycin, (D) pure paclitaxel, (E) CLA loaded CdS nanoparticles, (F) PTX loaded CdS nanoparticles, (G) CLA loaded NiO nanoparticles and (H) PTX loaded NiO nanoparticles. CLA: clarithromycin; PTX: paclitaxel; CdS: cadmium sulfide; NiO: nickel oxide

Differential scanning calorimetric (DSC)

The Differential Scanning Calorimetric (DSC) spectrum (fig. 5) of blank CdS and NiO nanoparticles display no sharp endothermic peak, while the DSC spectrum of free CLA displays a sharp narrow, intense endothermic peak at 228.58 °C that corresponds to the melting of the drug indicating its crystallinity [49] and decomposition of the drug after this temperature. The DSC spectrum of loaded CLA with CdS nanoparticles shows a small non-intense peak at 92.1 °C that indicates the initiation of melting of the complex and sharp, intense endothermic peak at 223.07 °C referring to melting of CLA followed by degradation of the compound. While the DSC spectrum of CLA-NiO complex displays sharp endothermic peak at 228.1 °C that indicates melting and finally degradation of the compound. The DSC spectrum of free paclitaxel shows sharp narrow endothermic peak at 217.65 °C that is attributed to the melting of the drug indicating its crystallinity [50], while the DSC spectrum obtained with PTX-CdS complex shows wide broad non-sharp endothermic peak at 109 °C that indicate the initiation of melting and another broad small endothermic peak at 165.04 °C corresponding to further melting and degradation of the new crystalline compound. The PTX-NiO complex shows DSC spectrum with multiple endothermic peak that appears as broad wide small peak at 163.8 °C that indicates the initiation of melting. Additionally, small intense peaks also appeared at 219.4, 245.54 and 256.68 °C indicating a shifting of free PTX melting peak and crystalline nature of new compound due to multiple endothermic peaks.

Atomic force microscopy (AFM)

The Atomic Force Microscopy (AFM) showed fine particle size distribution (fig. 6) of particles for clarithromycin loaded CdS and

NiO nanoparticles with smooth surfaces as shown in AFM images (fig. 7) in comparison with free CLA and blank CdS and NiO nanoparticles. The same was observed in paclitaxel, in which AFM images of loaded PTX with CdS and NiO nanoparticles show rice shaped particles with smooth surfaces and fine distribution than that of free PTX. The average particle size was also determined by AFM measurement, in which the average sizes of CLA loaded CdS and NiO nanoparticles were 125.51 and 98.85 nm respectively, that were higher than that of free CLA (74.99 nm), blank CdS nanoparticles (83.18 nm) and blank NiO nanoparticles (82.57 nm). The same was observed for paclitaxel, in which the average size of PTX before loading was 95.28 nm while the average sizes after loading with CdS and NiO nanoparticles were 116.7 nm and 106.03 nm respectively indicating drug loading of CLA and PTX with the CdS and NiO nanoparticles.

Yield, entrapment efficiency and drug loading percentages

The yield percentage of the reaction involving clarithromycin with CdS and NiO nanoparticles after complexation was 66.34% and 64.1% respectively. While the yield percentage of the reaction involving with paclitaxel-loaded CdS and NiO nanoparticles was 62.9% and 95.04% respectively. The drug content of clarithromycin and paclitaxel that has been loaded on CdS and NiO nanocarriers was expressed as percentage of drug loading, in which for CLA loaded CdS and NiO nanoparticles was 56.66% and 86.6% respectively and for PTX loaded CdS and NiO nanoparticles was 76.65% and 95.67% respectively. The percentage of clarithromycin that has been efficiently entrapped with CdS and NiO nanoparticles was 92.67% and 94.6% respectively while the percentage of entrapment efficiency for paclitaxel with CdS and NiO nanoparticles was 123.66% and 104% respectively.

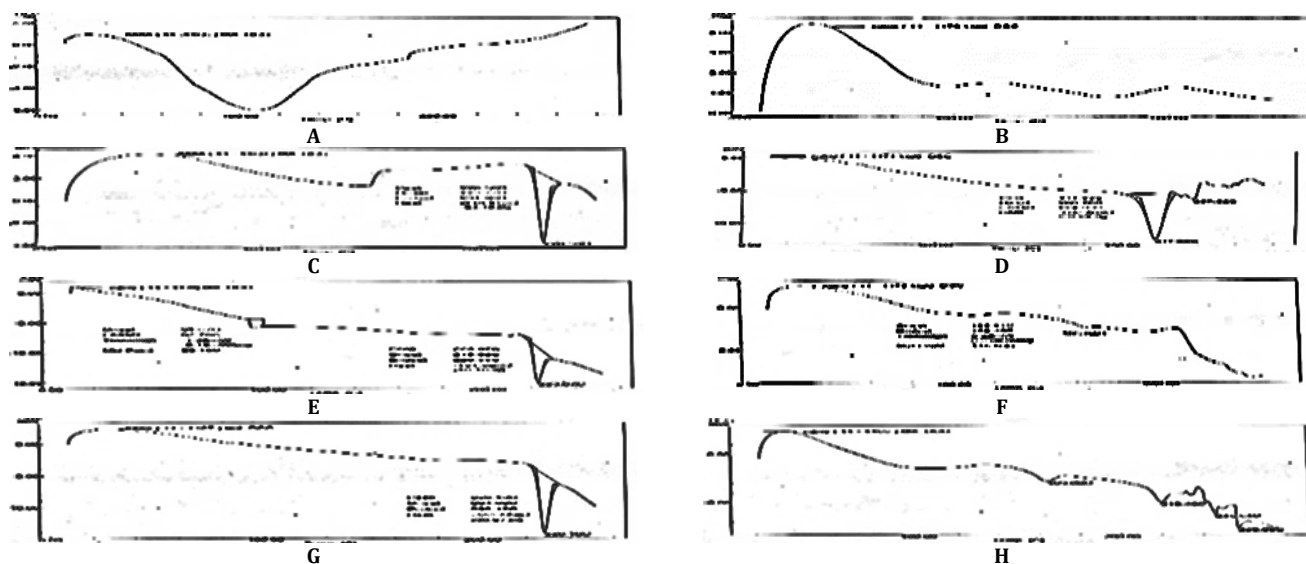


Fig. 5: DSC of (A) blank CdS nanoparticles, (B) blank NiO nanoparticles, (C) pure clarithromycin, (D) pure paclitaxel, (E) CLA loaded CdS nanoparticles, (F) PTX loaded CdS nanoparticles, (G) CLA loaded NiO nanoparticles and (H) PTX loaded NiO nanoparticles. CLA: clarithromycin; PTX: paclitaxel; CdS: cadmium sulfide; NiO: nickel oxide

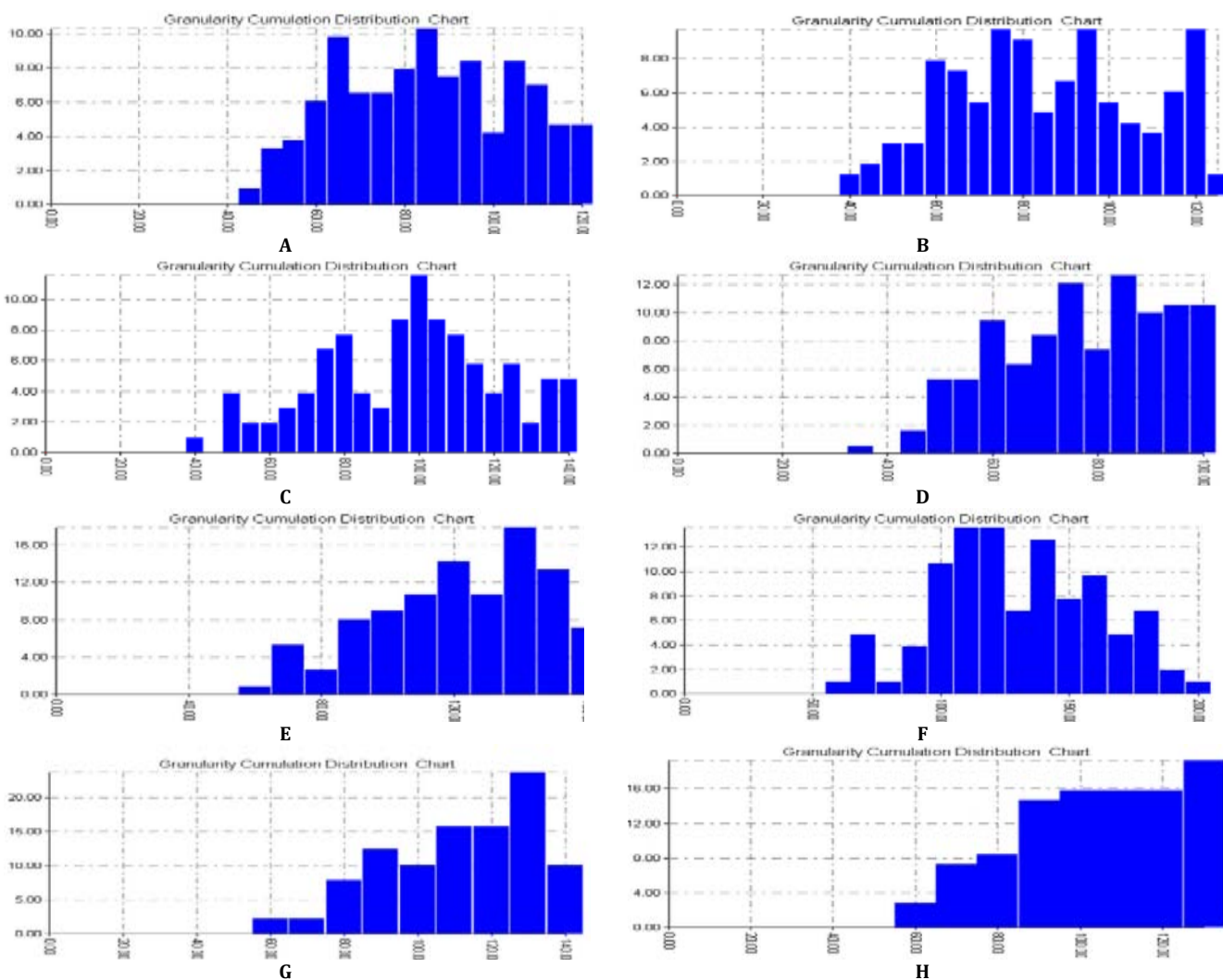


Fig. 6: AFM particle size distribution of (A) blank CdS nanoparticles, (B) blank NiO nanoparticles, (C) pure CLA, (D) pure PTX, (E) CLA loaded CdS nanoparticles, (F) PTX loaded CdS nanoparticles, (G) CLA loaded NiO nanoparticles and (H) PTX loaded NiO nanoparticles. CLA: clarithromycin; PTX: paclitaxel; CdS: cadmium sulfide; NiO: nickel oxide

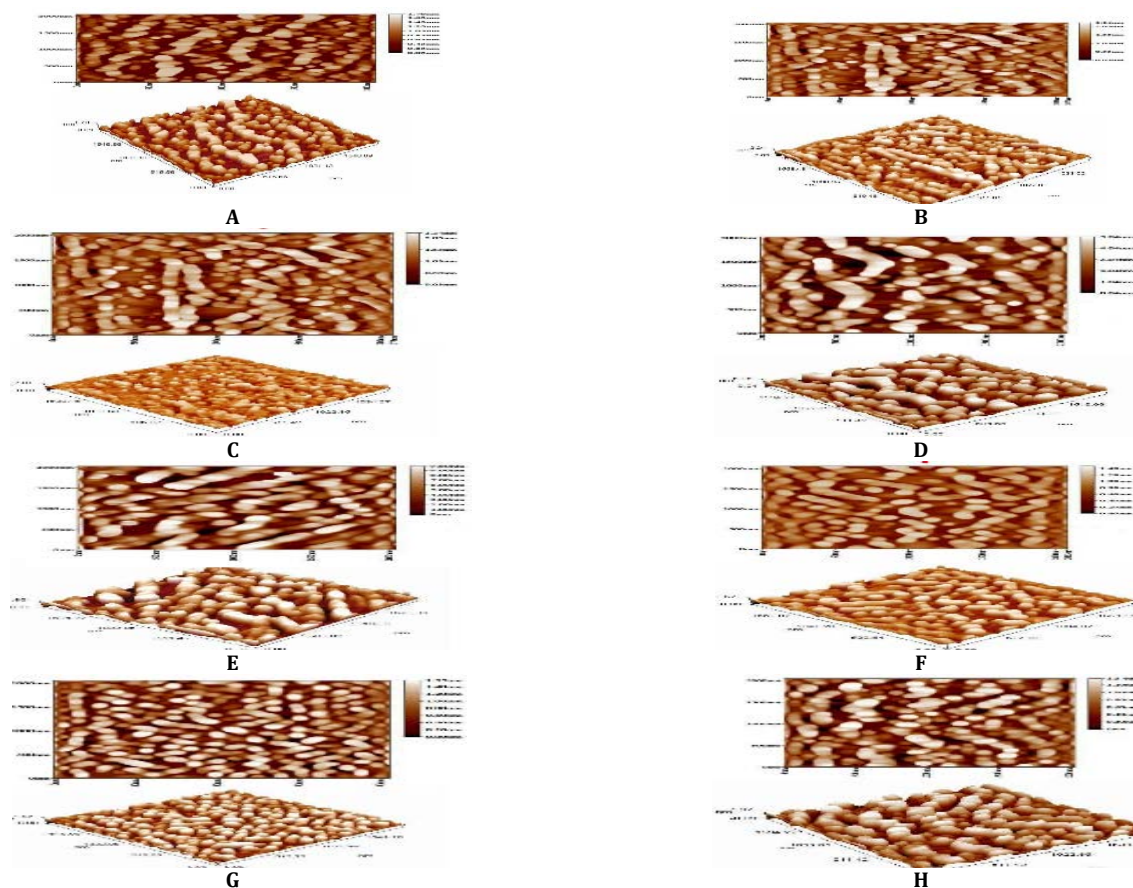


Fig. 7: AFM two and three dimensional images of (A) blank CdS nanoparticles, (B) blank NiO nanoparticles, (C) pure clarithromycin, (D) pure paclitaxel, (E) CLA loaded CdS nanoparticles, (F) PTX loaded CdS nanoparticles, (G) CLA loaded NiO nanoparticles and (H) PTX loaded NiO nanoparticles. CLA: clarithromycin; PTX: paclitaxel; CdS: cadmium sulfide; NiO: nickel oxide

Solubility determination of drugs before (free drug) and after loading with nanoparticles

The results are illustrated in (table 2) indicating that the solubility of clarithromycin loaded on CdS and NiO nanocarriers was significantly* improved in comparison with the saturated solubility of free CLA, while paclitaxel shows the non-significant difference in the saturated solubility after loading on CdS and NiO nanoparticles from that of unloaded PTX.

In vitro drugs release study

The *in vitro* release of clarithromycin (fig. 8) from drug loaded nanoparticles in comparison to pure CLA shows that the percentage

release of CLA after 30 min equal 34.1% from pure CLA, while the release after 30 min was found to be 49.86% and 88.95% from CLA-CdS and CLA-NiO complexes respectively. The release percentage of CLA reaches 100% from CdS and NiO nanoparticles within 150 and 45 min respectively, while pure CLA gave only 57% release within 150 min indicating significantly* faster dissolution and release of drug from CLA-NiO complex than that of CLA-CdS complex and both of them shows higher dissolution than pure drug.

No release profile was detected for paclitaxel from CdS and NiO nanocarriers as well as for pure PTX after 8 h due to very low solubility of the drug.

Table 2: Saturated solubility of clarithromycin and paclitaxel before and after loading with CdS and NiO nanoparticles

Sample	Solubility (mg/ml)
Clarithromycin	0.203±0.017
Clarithromycin loaded CdS nanoparticles	0.397±0.035
Clarithromycin loaded NiO nanoparticles	0.510±0.048
Paclitaxel	0.0145±0.0012
Paclitaxel loaded CdS nanoparticles	0.0127±0.0011
Paclitaxel loaded NiO nanoparticles	0.0112±0.0012

Saturated solubility data represent mean (±SD) (n=3). CdS: cadmium sulfide; NiO: nickel oxide

Antibacterial activity test of clarithromycin loaded nanoparticles

The antibacterial activity of clarithromycin loaded CdS and NiO nanoparticles in comparison with free CLA and blank nanoparticles (CdS and NiO) was determined by measuring the zone of inhibition

(ZOI) caused by each sample separately in Muller Hinton agar at 37 °C and 24 h incubation. The results illustrated in (table 3) where there was the non-significant difference in the activity of CLA before and after loading with CdS and NiO nanoparticles on Gram+ve bacteria *Staphylococcus aureus* and *Streptococcus pyogen* and on Gram-ve bacteria *Serratia marcescens*, while there is no effect on

Gram-ve bacteria *Klebsiella oxytoca*. Blank CdS nanoparticles showed no activity against all examined bacteria while NiO

nanoparticles showed antibacterial activity only against Gram+ve bacteria. The solvent used (DMSO) showed no effect in all samples.

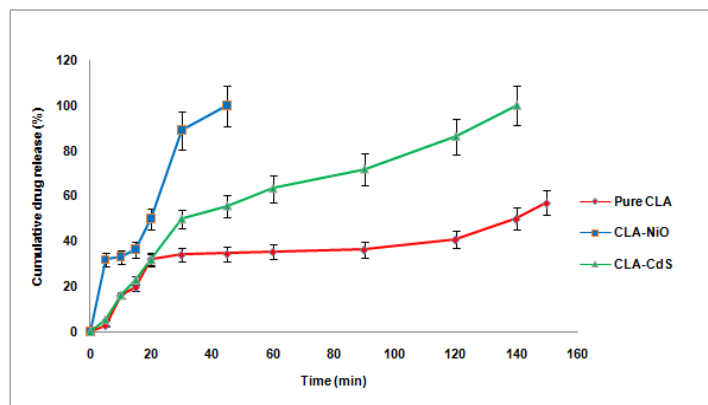


Fig. 8: Comparative *in vitro* release profile of pure clarithromycin, CLA loaded CdS nanoparticles and CLA loaded NiO nanoparticles in phosphate buffer solution (pH 7.4). Cumulative drug release percent data points represent mean(±SD) (n=3). CLA: clarithromycin; CdS: cadmium sulfide; NiO: nickel oxide

Table 3: Antibacterial activity of pure clarithromycin, clarithromycin loaded CdS and NiO nanoparticles and blank CdS and NiO nanoparticles represented by zone of inhibition (mm)

Sample	<i>Staphylococcus aureus</i>	<i>Streptococcus pyogen</i>	<i>Serratia marcescens</i>	<i>Klebsiella oxytoca</i>
Control (dimethyl sulfoxide)	-	-	-	-
Pure clarithromycin	31±2.5	32±2.6	20±1.8	-
Clarithromycin loaded CdS nanoparticles	32±3	34±3.1	20±1.5	-
Clarithromycin loaded NiO nanoparticles	32±2.8	35±3.3	22±2	-
CdS nanoparticles	-	-	-	-
NiO nanoparticles	20±1.7	16±1.2	-	-

Inhibition zone data represent mean(±SD) (n=3). CdS: cadmium sulfide; NiO: nickel oxide

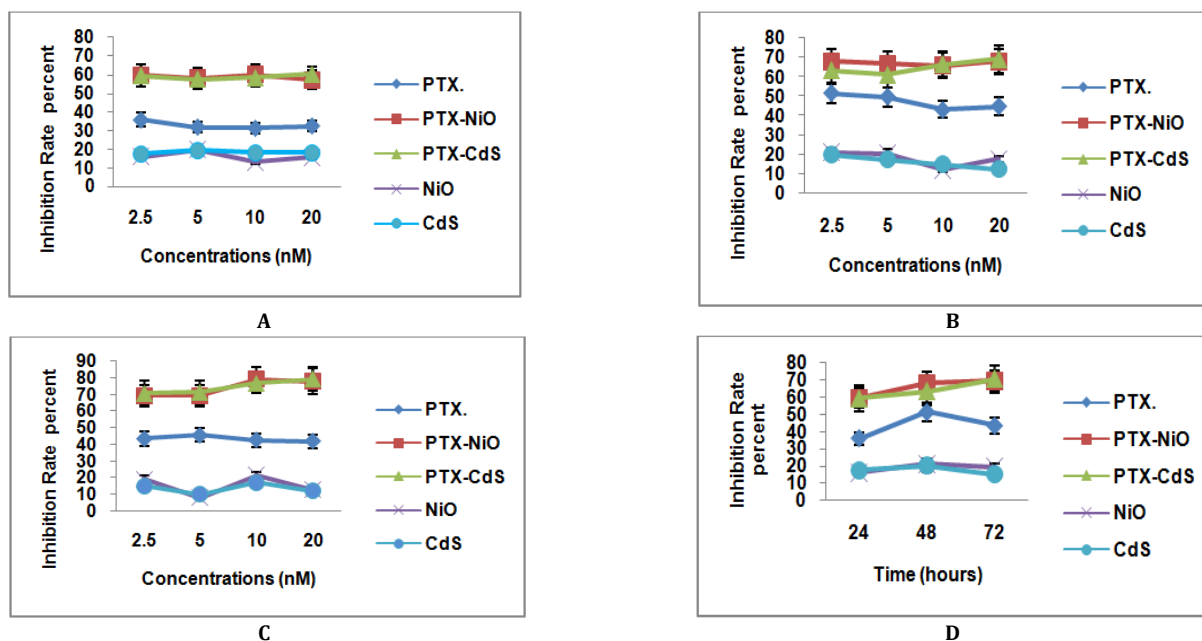


Fig. 9: Comparative *in vitro* cytotoxicity of pure paclitaxel, PTX loaded CdS nanoparticles, PTX loaded NiO nanoparticles, blank CdS nanoparticles and blank NiO nanoparticles showing the effect of concentration on their anticancer activity on MCF-7 cell line after (A) 24, (B) 48 and (C) 72 h of exposure, (D) Time-response curve for PTX using 2.5 nM concentration. Inhibition rate percent data points represent mean(±SD) (n=3). PTX: paclitaxel; CdS: cadmium sulfide; NiO: nickel oxide

Cytotoxic activity of paclitaxel-loaded nanoparticles

MCF-7 and MCF-10A cells were treated with increasing concentrations of paclitaxel before and after loading with CdS and NiO nanoparticles as well as with blank CdS and NiO nanoparticles where each sample was dissolved in dimethyl sulfoxide (DMSO), knowing that DMSO showed no or negligible cytotoxic activity (inhibition rate percent IR %) on both tumor and normal cells.

Paclitaxel from PTX loaded CdS and NiO nanocarriers shows significantly* higher cytotoxic effect (high IR %) than that of pure PTX and blank CdS and NiO nanoparticles on MCF-7 cancer cell line (fig. 9) in all concentrations used (2.5-20 nM) at different times of exposure (24, 48 and 72 h). The IR % for all concentrations of the same sample was almost the same indicating dose-independent

kinetic. In addition, there was the non-significant difference in the IR % between PTX loaded on CdS and on NiO nanoparticles. To evaluate the cytotoxic effect of paclitaxel loaded CdS and NiO nanoparticles on MCF-10A human mammary epithelial cell line (fig. 10) the same concentrations and times of exposure were applied. It was found that the undesirable cytotoxic effect of PTX loaded CdS and NiO nanoparticles on MCF-10A (normal human mammary epithelial cell line) were significant* lower than that of pure PTX and blank CdS and NiO nanoparticles from all used concentrations and at different times of exposure. Upon comparison with its cytotoxic activity on cancer cells, variable dose-kinetic was observed where above 2.5 nM variable changes observed including steep decline observed after 48 h, while after 72 h the steep decline was observed until 10 nM after which enhanced cytotoxicity was obtained.

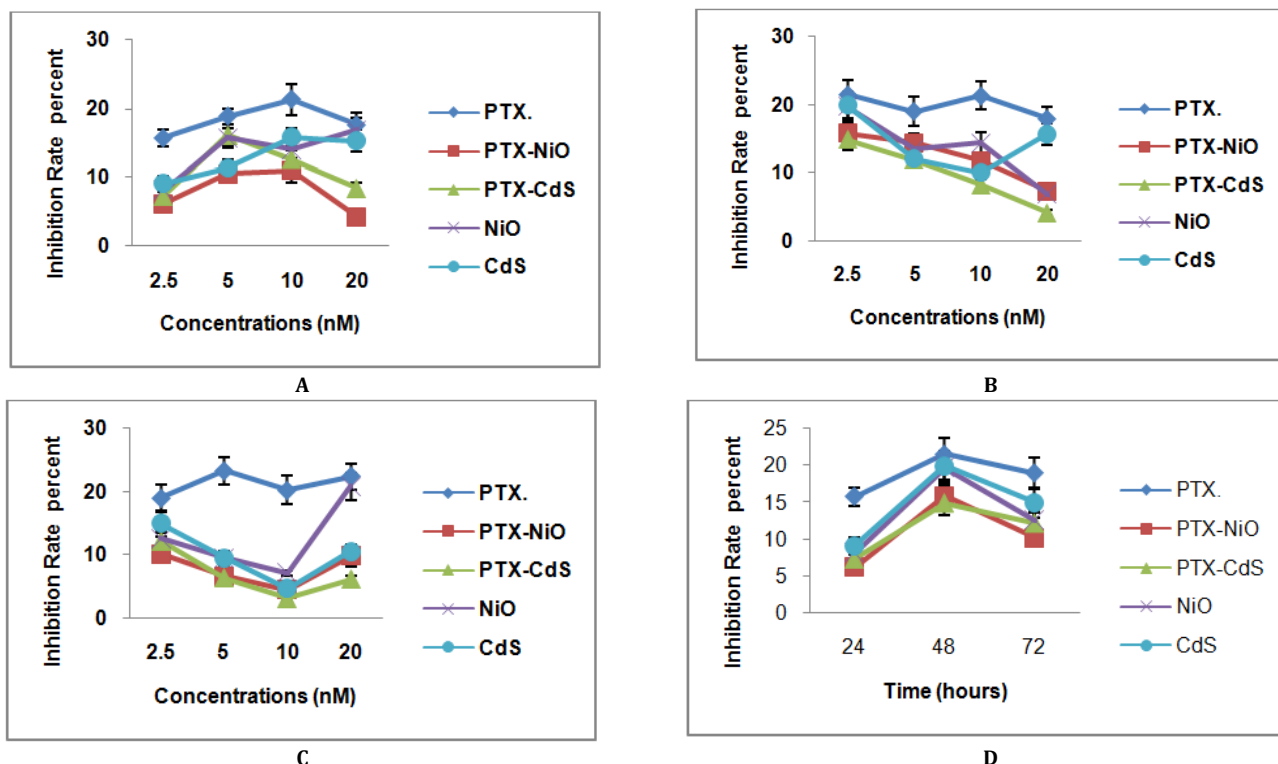


Fig. 10: Comparative *in vitro* cytotoxicity of pure paclitaxel, PTX loaded CdS nanoparticles, PTX loaded NiO nanoparticles, blank CdS nanoparticles and blank NiO nanoparticles showing the effect of concentration on their anticancer activity on MCF-10A cell line after (A) 24, (B) 48 and (C) 72 h of exposure, (D) Time-response curve for PTX using 2.5 nM concentration. Inhibition rate percent data points represent mean(±SD) (n=3). PTX: paclitaxel, CdS: cadmium sulfide, NiO: nickel oxide

DISCUSSION

The synthesis of clarithromycin/paclitaxel-CdS/NiO complexes was carried out using one-step reaction with high yield % indicating its simplicity and applicability. The loading of CLA and PTX on CdS and NiO nanoparticles was evaluated depending on changes in crystallinity, solubility, dissolution, particle size, morphology as well as their biological activities. The IR spectra (fig. 1) shows the same main functional groups of CLA and PTX before and after loading with CdS and NiO nanoparticles with small shifting, indicating physical complexes formation between each drug and nanocarriers rather than chemical interaction [36, 51, 52].

The smooth surfaces and fine distribution of drug-nanocarrier complexes than that of free CLA, free PTX and blank CdS and NiO nanoparticles showed by SEM and AFM (fig. 3, 6 and 7) indicate surface loading of drugs [52, 53] that accommodate also with the results obtained from TGA spectra (fig. 4), where TGA spectra of CLA after loading with CdS and NiO nanoparticles showed thermal weight loss peaks at 255.5 °C and 276 °C respectively that is close to the melting peak of free CLA at 279 °C, while TGA spectra of PTX

loaded CdS and NiO nanoparticles showed thermal weight loss peaks at 213.8 °C and 229.6 °C respectively that is also close to the melting peak of unloaded PTX at 230.9 °C [54, 55]. Additionally, the high % yield, % drug loading and % entrapment efficiency indicate high drug loading with the surface complex formation. Particle size increment that was detected by SEM and AFM measurements after loading of CLA and PTX on CdS and NiO nanoparticles in comparison with that of free drugs and blank nanoparticles (CdS and NiO) also confirm their loading [53, 56, 57].

The *in vitro* release of CLA from nanocarriers (fig. 8) was significantly* increased in comparison with free CLA, this increased dissolution and solubility could be caused by the phase transition from crystalline to amorphous structure that was approved with XRD and DSC spectra (fig. 2 and 5 respectively), where the XRD spectra of CLA after loading with CdS and NiO nanoparticles showed less characterized as well as less intense sharp peaks with decreased multiplicity in comparison with unloaded CLA indicating enhanced amorphous property [58], while the DSC spectra of CLA loaded CdS and NiO nanoparticles showed shorter crystalline endothermic peaks at 223.07 °C and 228.1 °C respectively than that of unloaded

CLA which showed longer more crystalline endothermic peak at 228.58 °C [41, 49, 59]. For PTX; the non-significant difference in its saturated solubility for pure PTX and loaded complexes, in addition to the undetectable release profile indicating the formation of more crystalline complexes that was also approved by XRD and DSC spectra (fig. 2 and 5 respectively), where the XRD spectrum of loaded drug showed enhanced multiplicity of diffraction peaks for both CdS and NiO complexes indicating more crystalline compounds obtained, while the DSC spectra of PTX loaded CdS (endothermic peaks at 109 °C and 165.04 °C) and NiO (endothermic peaks at 163.8, 219.4, 245.54 and 256.68 °C) nanoparticles showed more than one endothermic peak indicating more than one glass transition temperature and more crystallinity [57, 60, 61]. These results are indicating that the loading of PTX on CdS and NiO nanoparticles did not improve its solubility/dissolution profile.

To evaluate the effect of drug loading on CdS and NiO nanoparticles on the biological activity, the antibacterial activity of CLA loaded on CdS and NiO nanoparticles (table 3) showed non-significant improvement in comparison to the unloaded drug, although the loading process significantly* improve the solubility/dissolution profile of the drug.

The anticancer activity of PTX (fig. 9) against breast cancer cells (MCF-7) was significantly* improved upon loading on CdS and NiO nanoparticles in comparison with the free drug, although the metal nanoparticles showed limited anticancer activity indicating that the loading process led to improve the permeability of the drug through the tumor cells by providing more stable PTX loaded complexes [43, 60, 62] and/or due to sustained release manner of PTX from nanocarriers [63] in addition to the synergistic effect of CdS (.) NiO nanoparticles [64]. While the undesirable cytotoxic effect of loaded drug (fig. 10) on normal mammary epithelial cells (MCF-10A) was significantly* lower than that of pure PTX and CdS and NiO nanoparticles, this could be attributed to the increased resistance of normal cells toward PTX loaded on CdS and NiO nanoparticles.

CONCLUSION

This work presents simple one-step reaction for loading of CLA and PTX using CdS and NiO nanoparticles with high % yield and loading content that improve the solubility/dissolution profile of CLA significantly* with non-significant improvement of its antibacterial activity, while for PTX, a remarkable significant* improvement in its anticancer activity was obtained after loading with CdS and NiO nanoparticles, in addition to significant* reduction in its cytotoxic effect on normal cells indicating an improvement in targeting and selectivity of the drug which is very well known to have a wide range of side effects through improving its permeability into the cancer cells rather than normal cells, although non-significant improvement in solubility/dissolution profile was observed.

ACKNOWLEDGEMENT

This study was funded by college of pharmacy, Al-Mustansiriya University. The authors are grateful to Iraqi Ministry of science and technology for performing the analytical methods in this study.

CONFLICT OF INTERESTS

Authors declare no conflict of interest

REFERENCES

1. Qian WY, Sun DM, Zhu RR, Du XL, Liu H, Wang SL. pH-sensitive strontium carbonate nanoparticles as new anticancer vehicles for controlled etoposide release. *Int J Nanomed* 2012;7:5781-92.
2. Suri SS, Fenniri H, Singh B. Nanotechnology-based drug delivery systems. *J Occup Med Toxicol* 2007;2:1-6.
3. Hamouda IM. Current perspectives of nanoparticles in medical and dental biomaterials. *J Biomed Res* 2012;26:143-51.
4. Conde J, Doria G, Baptista P. Noble metal nanoparticles applications in cancer. *J Drug Delivery* 2012;2012:1-12.
5. Salvadori MR, Nascimento CAO, Corrêa B. Nickel oxide nanoparticles film produced by dead biomass of filamentous fungus. *Sci Rep* 2014;4:1-6.
6. Raj KP, Sivakarthish P, Uthirakumar A, Thangaraj V. Cytotoxicity assessment of synthesized nickel oxide nanoparticles on MCF-7 and A-549 cancer cell lines. *J Chem Pharm Sci* 2014;2014:269-71.
7. Shao L, Gao Y, Yan F. Semiconductor quantum dots for biomedical applications. *Sensors* 2011;11:11736-51.
8. Chen G, Yi B, Zeng G, Niu Q, Yan M, Chen A, et al. Facile green extracellular biosynthesis of CdS quantum dots by the white rot fungus *Phanerochaete chrysosporium*. *Colloids Surf B* 2014;117:199-205.
9. Wang LY, Wang L, Gao F, Yu ZY, Wu ZM. Application of functionalized CdS nanoparticles as fluorescence probe in the determination of nucleic acids. *Analyst* 2002;127:977-80.
10. Chen N, He Y, Su Y, Li X, Huang Q, Wang H, et al. The cytotoxicity of cadmium-based quantum dots. *Biomaterials* 2012;33:1238-44.
11. Hossain ST, Mukherjee SK. Toxicity of cadmium sulfide (CdS) nanoparticles against *Escherichia coli* and HeLa cells. *J Hazard Mater* 2013;260:1073-82.
12. Jain A, Gulbake A, Jain A, Shilpi S, Hurkat P, Kashaw S, et al. Development and validation of the HPLC method for simultaneous estimation of paclitaxel and topotecan. *J Chromatogr Sci* 2013;52:697-703.
13. Harisa GI. Blood viscosity as a sensitive indicator for paclitaxel-induced oxidative stress in human whole blood. *Saudi Pharm J* 2015;23:48-54.
14. Khadka P, Ro J, Kim H, Kim I, Kim JT, Kim H, et al. Pharmaceutical particle technologies: An approach to improve drug solubility, dissolution, and bioavailability. *Asian J Pharm Sci* 2014;9:304-16.
15. Yang FH, Zhang Q, Liang QY, Wang SQ, Zhao BX, Wang YT, et al. Bioavailability enhancement of paclitaxel via a novel oral drug delivery system: paclitaxel-loaded glycyrrhizic acid micelles. *Molecules* 2015;20:4337-56.
16. Patingrao DL, Kadu P. Formulation and evaluation of clarithromycin gastro retentive dosage form. *J Chem Pharm Res* 2014;6:82-9.
17. Adzitey F. Antibiotic classes and antibiotic susceptibility of bacterial isolates from selected poultry; a mini review. *World Vet J* 2015;5:36-41.
18. Morakul B, Suksiriworapong J, Leanpolchareanchai J, Junyaprasert VB. Precipitation-lyophilization-homogenization (PLH) for the preparation of clarithromycin nanocrystals: influencing factors on physicochemical properties and stability. *Int J Pharm* 2013;457:187-96.
19. Rao BS, Kumar BR, Reddy VR, Rao TS. Preparation and characterization of CdS nanoparticles by chemical coprecipitation technique. *Chalcogenide Lett* 2011;8:177-85.
20. Adekunle AS, Oyekunle JA, Oluwafemi OS, Joshua AO, Makinde WO, Ogunfowokan AO, et al. Comparative catalytic properties of Ni (OH) 2 and NiO nanoparticles towards the degradation of nitrite (NO₂-) and nitric oxide (NO). *Int J Electrochem Sci* 2014;9:3008-21.
21. Mohammadjooa M, Khorshidia ZN, Sadrnezhad S, Mazinan V. Synthesis and characterization of nickel oxide nanoparticle with wide band gap energy prepared via thermochemical processing. *Nanosci Nanotechnol: Int J* 2014;4:6-9.
22. Ranjiit K, AbdulBaquee A. Nanoparticle: an overview of preparation, characterization, and application. *Int Res J Pharm* 2013;4:47-57.
23. Liggins R, Burt H. Polyether-polyester diblock copolymers for the preparation of paclitaxel loaded polymeric micelle formulations. *Adv Drug Delivery Rev* 2002;54:191-202.
24. Sekar RP, Elango K, Damayanthi D, Saranya JS. Formulation and evaluation of azathioprine loaded silver nanoparticles for the treatment of rheumatoid arthritis. *Asian J Biomed Pharm Sci* 2013;3:28-32.
25. Bykkam S, Ahmadipour M, Narisngam S, Kalagadda VR, Chidurala SC. Extensive studies on X-Ray diffraction of green synthesized silver nanoparticles. *Adv Nanopart* 2015;4:1-10.
26. Heera P, Shanmugam S. Nanoparticle characterization and application: an overview. *Int J Curr Microbiol Appl Sci* 2015;4:379-86.
27. Pal SL, Jana U, Manna P, Mohanta G, Manavalan R. Nanoparticle: an overview of preparation and characterization. *J Appl Pharm Sci* 2011;1:228-34.

28. Elias A, Crayton SH, Warden-Rothman R, Tsourkas A. Quantitative comparison of tumor delivery for multiple targeted nanoparticles simultaneously by multiplex ICP-MS. *Sci Rep* 2014;4:1-9.
29. Sierra-Ávila R, Pérez-Alvarez M, Cadenas-Pliego G, Padilla VC, Ávila-Orta C, Camacho OP, *et al.* Synthesis of copper nanoparticles using a mixture of allylamine and polyallylamine. *J Nanomater* 2015;2015:1-9.
30. El-Zaher NA, Melegy MS, Guirguis OW. Thermal and structural analyses of PMMA/TiO₂ nanoparticles composites. *Nat Sci* 2014;6:859-70.
31. Bande F, Arshad SS, Hair Bejo M, Abdullahi Kamba S, Omar AR. Synthesis and characterization of chitosan-saponin nanoparticle for application in plasmid DNA delivery. *J Nanomater* 2015;2015:1-8.
32. Chan JC, Hannah-Moore N, Rananavare SB. Controlled deposition of tin oxide and silver nanoparticles using microcontact printing. *Crystals* 2015;5:116-42.
33. Moosa AA, Ridha AM, Al-Kaser M. Process parameters for green synthesis of silver nanoparticles using leaves extract of *Aloe Vera* plant. *Int J Multidisciplinary Curr Res* 2015;3:966-75.
34. Filippousi M, Papadimitriou SA, Bikiaris DN, Pavlidou E, Angelakeris M, Zamboulis D, *et al.* Novel core-shell magnetic nanoparticles for Taxol encapsulation in biodegradable and biocompatible block copolymers: Preparation, characterization and release properties. *Int J Pharm* 2013;448:221-30.
35. Gavini V, Murthy MS, Kumar PK. Formulation and *in vitro* evaluation of nanoparticulate drug delivery system loaded with 5-fluorouracil. *Res J Pharm Dosage Forms Technol* 2014;6:243-8.
36. Shahbazinia M, Foroutan SM, Bolourchian N. Dissolution rate enhancement of clarithromycin using ternary ground mixtures: nanocrystal formation. *Iran J Pharm Res* 2013;12:587-98.
37. Pandey S, Kumar S. Evaluation of the effect of hydrophilic polymer blend to extend the release of clarithromycin from prepared microcapsules. *J Pharm Sci Res* 2010;2:759-66.
38. Ahmad J, Mir SR, Kohli K, Chuttani K, Mishra AK, Panda A, *et al.* Solid-nanoemulsion preconcentrate for oral delivery of paclitaxel: formulation design, biodistribution, and γ scintigraphy imaging. *BioMed Res Int* 2014;2014:1-12.
39. Elsayed I, Abdelbary AA, Elshafeey AH. Nanosizing of a poorly soluble drug: technique optimization, factorial analysis, and pharmacokinetic study in healthy human volunteers. *Int J Nanomed* 2014;9:2943-53.
40. Valizadeh H, Mohammadi G, Ehyaei R, Milani M, Azhdarzadeh M, Zakeri-Milani P, *et al.* Antibacterial activity of clarithromycin loaded PLGA nanoparticles. *Pharmazie* 2012;67:63-8.
41. Ramezani V, Vatanara A, Najafabadi AR, Moghaddam SPH. Clarithromycin dissolution enhancement by preparation of aqueous nanosuspensions using so no precipitation technique. *Iran J Pharm Res* 2014;13:809-18.
42. Wang L, Li H, Wang S, Liu R, Wu Z, Wang C, *et al.* Enhancing the antitumor activity of berberine hydrochloride by solid lipid nanoparticle encapsulation. *AAPS PharmSciTech* 2014;15:834-44.
43. Adesina SK, Holly A, Kramer-Marek G, Capala J, Akala EO. Polylactide-based paclitaxel-loaded nanoparticles fabricated by dispersion polymerization: characterization, evaluation in cancer cell lines, and preliminary biodistribution studies. *J Pharm Sci* 2014;103:2546-55.
44. Liebmann J, Cook J, Lipschultz C, Teague D, Fisher J, Mitchell J. Cytotoxic studies of paclitaxel (Taxol) in human tumour cell lines. *Br J Cancer* 1993;68:1104-9.
45. Lin Y, Jiang D, Li Y, Han X, Yu D, Park JH, *et al.* Effect of sun ginseng potentiation on epirubicin and paclitaxel-induced apoptosis in human cervical cancer cells. *J Ginseng Res* 2015;39:22-8.
46. Prasath M, Arun RB, Revathy R. Synthesis and characterization of Mn²⁺-doped CdS nanoparticles. *J Chem Pharm Res* 2015;7:875-85.
47. Kishore N, Mukherjee S. Synthesis, and characterization of mixed ferrites. *Int J Sci Res Publications* 2014;4:1-5.
48. Honary S, Zahir F. Effect of zeta potential on the properties of nano-drug delivery systems-a review (Part 2). *Trop J Pharm Res* 2013;12:265-73.
49. Zakeri-Milani P, Islambulchilar Z, Majidpour F, Jannatabadi E, Lotfipour F, Valizadeh H. A study on enhanced intestinal permeability of clarithromycin nanoparticles. *Braz J Pharm Sci* 2014;50:121-9.
50. Bhoskar M, Patil P. Develop and evaluation of paclitaxel-loaded nanoparticles using 24 factorial design. *Int J Curr Pharm Res* 2015;7:64-72.
51. Zhao Z, Li Y, Zhang Y. Preparation and characterization of paclitaxel loaded SF/PLLA-PEG-PLLA nanoparticles via solution-enhanced dispersion by supercritical CO₂. *J Nanomater* 2015;2015:1-7.
52. Hiremath JG, Khamar NS, Palavalli SG, Rudani CG, Aitha R, Mura P. Paclitaxel-loaded carrier based biodegradable polymeric implants: preparation and *in vitro* characterization. *Saudi Pharm J* 2013;21:85-91.
53. Derman S, Mustafaeva ZA, Abamor ES, Bagirova M, Allahverdiyev A. Preparation, characterization and immunological evaluation: canine parvovirus synthetic peptide loaded PLGA nanoparticles. *J Biomed Sci* 2015;22:1-12.
54. Smitha K, Anitha A, Furuike T, Tamura H, Nair SV, Jayakumar R. *In vitro* evaluation of paclitaxel loaded amorphous chitin nanoparticles for colon cancer drug delivery. *Colloids Surf B* 2013;104:245-53.
55. Ganesh M, Ubaidulla U, Hemalatha P, Peng MM, Jang HT. Development of duloxetine hydrochloride loaded mesoporous silica nanoparticles: characterizations and *in vitro* evaluation. *AAPS PharmSciTech* 2015;16:944-51.
56. Tuncer Degim I, Kadioglu D. Cheap, suitable, predictable and manageable nanoparticles for drug delivery: quantum dots. *Curr Drug Delivery* 2013;10:32-8.
57. Martins KF, Messias AD, Leite FL, Duek EA. Preparation and characterization of paclitaxel-loaded PLDLA microspheres. *Mater Res* 2014;17:650-6.
58. Kumar A, Singh N, Kaushik D. Taste masking of clarithromycin using complexation with ion exchange resin. *Int J PharmTech Res* 2014;6:203-11.
59. Thadkala K, Nanam PK, Rambabu B, Sailu C, Aukunuru J. Preparation and characterization of amorphous ezetimibe nanosuspensions intended for enhancement of oral bioavailability. *Int J Pharm Invest* 2014;4:131-7.
60. Esfandyari-Manesh M, Mostafavi SH, Majidi RF, Koopaei MN, Ravari NS, Amini M, *et al.* Improved anticancer delivery of paclitaxel by albumin surface modification of PLGA nanoparticles. *DARU J Pharm Sci* 2015;23:1-8.
61. Onishi Y, Eshita Y, Ji RC, Onishi M, Kobayashi T, Mizuno M, *et al.* Anticancer efficacy of a supramolecular complex of a 2-diethylaminoethyl-dextran-MMA graft copolymer and paclitaxel used as an artificial enzyme. *Beilstein J Nanotechnol* 2014;5:2293-307.
62. Ma P, Mumper RJ. Paclitaxel nano-delivery systems: a comprehensive review. *J Nanomed Nanotechnol* 2013;4:1-35.
63. Tang X, Cai S, Zhang R, Liu P, Chen H, Zheng Y, *et al.* Paclitaxel-loaded nanoparticles of star-shaped cholic acid-core PLA-TPGS copolymer for breast cancer treatment. *Nanoscale Res Lett* 2013;8:1-12.
64. Vinardell Martínez-Hidalgo MP, Mitjans Arnal M. Antitumor activities of metal oxide nanoparticles. *Nanomaterials* 2015;5:1004-21.